ELSEVIER

Mechanics of Materials 31 (1999) 381–393

MECHANICS OF MATERIALS

www.elsevier.com/locate/mechmat

A paraboloid failure surface for transversely isotropic materials

O. Cazacu, N.D. Cristescu *

Department of Aerospace Engineering, Mechanics and Engineering Science, University of Florida, P.O. Box 116250, Gainesville, FL 32611-6250, USA

Received 20 February 1998

Abstract

An invariant 3-D failure criterion for transversely isotropic solids is presented. For isotropic conditions, this criterion reduces to Mises–Schleicher failure criterion. It is shown that the anisotropic Mises–Schleicher (AMS) criterion can accurately describe the observed failure characteristics of transversely isotropic rocks under both compressive and tensile stresses. This criterion predicts that the application of multiaxial tensile stresses on rock reduces the value of the failure strength, i.e., the predicted value of the hydrostatic tensile strength as well as of the biaxial tensile strength is less than the uniaxial tensile strength in any direction. The intersections of the AMS failure surfaces with the octahedral plane demonstrates the ability of the criterion to describe the directional character of the strength of transversely isotropic materials under general loading conditions. The application of this criterion to conventional triaxial compression, reduced triaxial extension, and biaxial conditions, shows that this criterion captures the influence of the magnitude of the intermediate principal stress on strength. Representative sets of data from tests on rock have been analyzed and comparison between the theoretical predictions and the data appears to be quite good with the accuracies generally within the natural scatter of test data. In this paper, the AMS criterion is applied to rock materials; however, it can be used to describe the strength anisotropy of any material exhibiting transverse isotropy.

Keywords: Transverse isotropy; Elliptic paraboloid failure surface; Strength differential effect; Rock

1. Introduction

In many rocks, due to the existence of well-defined fabric elements such as bedding, layering, foliation or lamination planes, or due to the existence of linear structures, anisotropy in brittle behavior can be important. The symmetries most frequently encountered are: transverse isotropy and orthotropy. By adopting both theoretical and experimental approaches, many authors have investigated the effect of the presence within the rock of pronounced anisotropic feature on strength. For rocks exhibiting intrinsic transverse isotropy, experimental studies have been performed mainly on cylindrical specimens subjected to axisymmetric state of compressive stresses. It has been found that the compressive strength of the rock varies significantly with the orientation of the maximum principal stress towards the preferential planes, and with the magnitude of the confining pressure (e.g., Allirot and Boehler, 1979; Attewell and

* Corresponding author. E-mail: ndc@AeMES.aero.ufl.edu.

0167-6636/99/$ – see front matter
PII: S0167-6636(99)00008-3

Sandford, 1974; Chenevert and Gatlin, 1965; Donath, 1964, 1972; Homand et al., 1993; Niandou, 1994; Ramamurthy, 1993, etc.). Indirect tensile tests, such as the Brazilian test, are commonly used to determine the tensile strength of isotropic rocks. However, they are not appropriate for anisotropic rock, since in this type of test the state of stress is not statically determinate but depends on the constitutive law of the rock, which is a priori unknown. On the other hand, direct tensile tests are very difficult to carry out. This is because both the bending stresses, or torsion moment (caused by the eccentricity of machine axial loads) and the anomalous concentrated stresses (induced by an improper connection between the ends of the specimen and the machine caps serving to transfer the tensile loads to the specimen) are frequently unavoidable (Nova and Zaninetti, 1990). Few direct tensile test results on intact transversely isotropic rocks have been reported in the literature (Nova and Zaninetti, 1990; Liao et al., 1997, etc.). Although much scatter exists in the measured limit stresses, a clear trend was observed: the tensile strength tends to increase regularly with the inclination of the planes of symmetry with respect to the horizontal. Failure criteria that accounts for the continuous variation of the compressive strength with orientation for transversely isotropic intact rock have been developed by several authors (e.g., Jaeger, 1960; McLamore and Gray, 1967; Ramamurthy, 1993, etc.). These criteria are simple in concept and in expression, and they provide good approximations for the strength under axisymmetric loading conditions. However, these theories require a large amount of curve fitting, and cannot be applicable to truly 3-D stress states. A more general approach was followed by Pariseau (1972). To take into account the possibility of unequal tensile and compressive strengths, and to describe the effect of the hydrostatic stress on strength, Pariseau extended Hill's criterion (Hill, 1948) by including a linear term in σ_{11}, σ_{22} and σ_{33}. A general theory of the flow and fracture of anisotropic solids was developed by Boehler (1978, 1987) and Boehler and Sawczuk (1977), in the framework of the theory of invariance. Nova (1980) has proposed a generalized failure condition that describes the failure of transversely isotropic rocks in compression. Subsequently, Nova and Zaninetti (1990) have developed an anisotropic strength criterion for tensile failure similar, conceptually, to the failure criterion for compression. However, no attempt has been made at developing a failure surface that is continuous in the stress space. Theocaris (1991) proposed an elliptic paraboloid failure criterion that accounts for the differential strength effect. This criterion was applied to a great number of transversely isotropic materials such as: fiber-reinforced composites, cellular solids, and brittle foams. An invariant formulation of a failure criterion for transversely isotropic solids was proposed by Cazacu et al. (1998). For isotropic conditions, this criterion reduces to the Mises–Schleicher criterion.

In this paper, the characteristic properties of this type of failure surface are further investigated. The intersections of the failure surfaces corresponding to arbitrary orientation of the principal stress system with respect to the structural system, by the octahedral plane are presented. It is thus shown that the criterion is able to describe the directional character of strength under general loading conditions. The application of the criterion to conventional triaxial compression, reduced triaxial extension, and biaxial conditions, shows the ability of the criterion to capture the influence of the magnitude of the intermediate principal stress on strength. Finally, comparisons between theoretical predictions and strength data on various transversely anisotropic rocks are presented.

2. The anisotropic Mises–Schleicher failure criterion

A general macroscopic failure criterion for transversely isotropic solids has been developed by Cazacu et al. (1998). As the derivation and formulation of the criterion has been described in detail in the paper mentioned, we shall just briefly recall it here for clarity. The anisotropic Mises–Schleicher (AMS) criterion is expressed as follows:

$$\frac{3}{2}\mathrm{tr}(\Sigma')^2 - \frac{m}{3}\mathrm{tr}\,\Sigma - 1 = 0, \tag{1}$$

with

$$\Sigma_{ij} = B_{ijkl}\sigma_{kl}. \tag{2}$$

In Eq. (1) prime stands for deviator, 'tr' denotes the trace operator, σ is the Cauchy stress tensor, and m is a material constant. The anisotropy is introduced by means of the fourth order tensor $\boldsymbol{B}$ that satisfies the usual symmetry conditions:

$$B_{ijkl} = B_{jikl} = B_{klij} = B_{ijlk}. \tag{3}$$

For given environmental conditions (e.g., temperature, humidity, etc.) $\boldsymbol{B}$ is supposed to be constant. In contrast to other existing criteria, the only restriction imposed on $\boldsymbol{B}$ is to be invariant under any orthogonal transformation belonging to the symmetry group of the material. Thus, in the structural coordinate system (S_1, S_2, S_3) associated with the material symmetries, the truncated matrix of $\boldsymbol{B}$ is:

$$B = \begin{bmatrix} a & b & b & 0 & 0 & 0 \\ b & d & e & 0 & 0 & 0 \\ b & e & d & 0 & 0 & 0 \\ 0 & 0 & 0 & \frac{d-e}{2} & 0 & 0 \\ 0 & 0 & 0 & 0 & \frac{c}{2} & 0 \\ 0 & 0 & 0 & 0 & 0 & \frac{c}{2} \end{bmatrix}, \tag{4}$$

where a, b, c, d and e are independent material parameters, and (S_2, S_3) defines the symmetry plane.For isotropic conditions, the proposed criterion reduces to the Mises–Schleicher paraboloid surface (see, e.g., Lubliner, 1990):

$$3J_2 + (\sigma_C - \sigma_T)I_1 - \sigma_T\sigma_C = 0, \tag{5}$$

where $J_2 = (1/2)[\mathrm{tr}(\sigma')^2]$, $I_1 = \mathrm{tr}(\sigma)$, and σ_T, σ_C are the tensile and compressive strength, respectively. In the structural system (S_1, S_2, S_3), the AMS criterion is expressed by:

$$\begin{aligned} &a_1\sigma_{11} + a_2(\sigma_{22} + \sigma_{33}) + A_{11}\sigma_{11}^2 + A_{22}(\sigma_{22}^2 + \sigma_{33}^2) \\ &+ 2A_{12}\sigma_{11}(\sigma_{22} + \sigma_{33}) + 2A_{23}\sigma_{22}\sigma_{33} + A_{44}\sigma_{23}^2 \\ &+ A_{55}(\sigma_{12}^2 + \sigma_{13}^2) = 1, \end{aligned} \tag{6}$$

where the coefficients in Eq. (6) are given by:

$$\begin{aligned} a_1 &= 1/3[-m(a+2b)], \\ a_2 &= 1/3[-m(b+e+d)], \\ A_{11} &= (a-b)^2, \\ A_{22} &= 1/2\left[(b-e)^2 + (d-e)^2 + (b-d)^2\right], \\ A_{44} &= 3(d-e)^2, \\ A_{55} &= 3c^2, \\ A_{23} &= A_{22} - A_{44}/2, \\ A_{12}^2 &= 1/2[A_{11}(A_{22} + A_{23})]. \end{aligned} \tag{7}$$

The physical interpretation of the parameters of the criterion may be revealed from simple laboratory tests: shear tests in the (S_2, S_3) plane and in the (S_1, S_2) plane, and uniaxial tests along the S_1 and the S_2 axis, respectively. Thus:

$$\begin{aligned} a_1 &= 1/X_C - 1/X_T, \\ a_2 &= 1/Y_C - 1/Y_T, \\ A_{11} &= 1/(X_T X_C), \\ A_{22} &= 1/(Y_T Y_C), \\ A_{44} &= 1/Q^2, \\ A_{23} &= A_{22} - A_{44}/2, \\ A_{55} &= 1/R^2. \end{aligned} \tag{7'}$$

Here, and throughout the text the compressive stresses are taken positive, X_C and $(-X_T)$ are the uniaxial compressive and tensile strengths along S_1, while Y_C and $(-Y_T)$ are the uniaxial compressive and tensile strengths along S_2; Q is the shear strength in the symmetry plane (S_2, S_3) while R denotes the shear strength in the (S_1, S_2) plane. It was shown (see Cazacu et al., 1998) that the additional condition: $1/Q^2 = 4/(Y_T Y_C) - 1/X_C$ ensures that in the three-dimensional space of the principal stresses the failure surface is an elliptic paraboloid for any orientation θ of the principal stresses system (X_1, X_2, X_3) with respect to the structural system (S_1, S_2, S_3) (see Fig. 1). It is worthwhile to note that in the AMS criterion the interaction coefficients A_{12}, and A_{23} are interrelated with the diagonal components A_{11}, A_{22}, and A_{44}, thus they are directly defined in terms of the basic engineering strengths of the material. This is a significant advantage, in determining the constitutive parameters, of the AMS criterion over most existing failure criteria. As an example, in Tsai and Wu, 1971 criterion, the determination of the off-diagonal coefficient F_{12} (i.e., the coefficient of $\sigma_{11}\sigma_{22}$ in the expression of the criterion in the structural coordinate system) has been found to be very sensitive and dependent on the nature of the

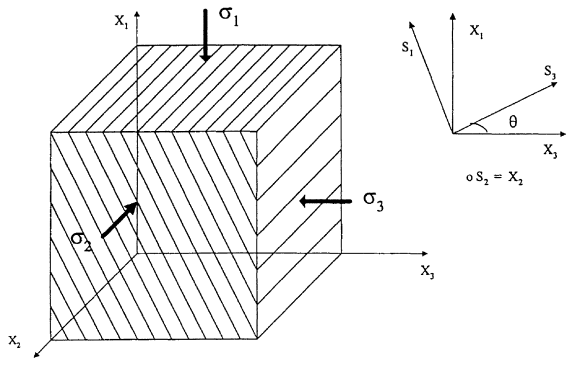

Fig. 1. Geometry of the problem: (X_1, X_2, X_3) – principal stresses system, and (S_1, S_2, S_3) – structural system.

particular test used for its determination. To overcome the difficulties related to the optimal experimental evaluation of F_{12} several definitions have been proposed (see Tsai and Hahn, 1980; Cowin, 1979; Wu and Stachurski, 1984). However, estimating the value of F_{12} is still a debated question (Labossière and Neale, 1987).

3. Shape of the AMS failure surface in principal stress space

To better understand the characteristic properties of the AMS failure surface, it is useful to represent it in: (1) the octahedral plane, (2) the triaxial plane, and (3) the biaxial plane.

3.1. The AMS failure surface in the deviatoric πplane ($\sigma_1+\sigma_2+\sigma_3=0$)

First, let us study the characteristics of the failure surface in the octahedral plane: $\sigma_1+\sigma_2+\sigma_3=0$. The case of one of the principal stress axes, the σ_2-axis say, coinciding with the structural axis S_2 whereas the two other stress axes rotate about S_2 with an angle θ, will be analyzed (see Fig. 1). Consider the $Oxyz$ frame related to the principal stress direction frame by the following relations:

$$x=\frac{1}{\sqrt{3}}(\sigma_1+\sigma_2+\sigma_3),\quad y=\frac{1}{\sqrt{2}}(\sigma_2-\sigma_1),$$
$$z=\frac{1}{\sqrt{6}}(-\sigma_1-\sigma_2+2\sigma_3). \tag{8}$$

The Ox-axis coincides with the hydrostatic axis ($\sigma_1=\sigma_2=\sigma_3$), hence the Oyz-plane coincides with the octahedral plane, whereas Oy is the bisector of $\sphericalangle(\sigma_2,-\sigma_1)$. In the $Oxyz$-frame, the equation of the AMS elliptic paraboloid is given by:

$$Ay^2+2hyz+Bz^2+2Gy+2Fz+Ix+c=0, \tag{9}$$

where

$$\begin{aligned}
A &= (1/2)\Big[(2A_{11}+A_{22}-A_{55})(\cos\theta)^4\\
&\quad +(A_{55}+A_{11}-4A_{22})(\cos\theta)^2+4A_{22}-A_{11}\Big],\\
h &= (\sqrt{3}/2)\Big[(2A_{11}+A_{22}-A_{55})(\cos\theta)^2\\
&\quad -A_{11}-2A_{22}+A_{55}\Big](\cos\theta)^2,\\
B &= (3/2)\Big[(2A_{11}+A_{22}-A_{55})(\cos\theta)^4\\
&\quad +(A_{55}-3A_{11})(\cos\theta)^2+A_{11}\Big],\\
G &= -(\sqrt{2}/4)(a_1-a_2)(\cos\theta)^2,\\
F &= -(\sqrt{6}/12)(a_1-a_2)(3(\cos\theta)^2-2),\\
I &= (\sqrt{3}/3)(a_1+2a_2),\\
c &= -1.
\end{aligned} \tag{10}$$

The intersection of any of the AMS surfaces (9) by the octahedral plane ($x=0$) is an ellipse. Indeed, to determine the nature of the conic of intersection, the following quantities need to be evaluated:

$$\Delta=\begin{bmatrix} A & h & G\\ h & B & F\\ G & F & -1\end{bmatrix},\quad J=AB-h^2,\quad I=A+B. \tag{11}$$

From Eq. (10) we get:

$$\begin{aligned}
I &= (1/2)(A_{44}+3A_{11}-\alpha(\sin 2\theta)^2),\\
J &= (3/4)\Big[A_{11}A_{44}(2(\cos\theta)^2-1)^2\\
&\quad +A_{55}(\sin\theta)^2(\cos\theta)^2(A_{44}+A_{11})\Big],\\
\Delta &= \beta+(1/4)\gamma(\sin 2\theta)^2,\\
\alpha &= (1/4)(9A_{11}+A_{44}-4A_{55}),\\
\beta &= (1/12)\Big\{-A_{44}\Big[9A_{11}+(a_1-a_2)^2\Big]\Big\},\\
\gamma &= (1/12)\Big\{-48\beta\\
&\quad -A_{55}\Big[9(A_{11}+A_{44})+(a_1-a_2)^2\Big]\Big\}.
\end{aligned} \tag{12}$$

Since $(\sin 2\theta)^2 \leqslant 1$ for any θ, it follows that: $I \geqslant (3A_{11} + 3A_{44} + 4A_{55})/8$, and $\Delta \leqslant \beta + \gamma/4 < -A_{55}[(a_1 - a_2)^2 + 9(A_{11} + A_{44})]/48$. Thus, for any θ: $\Delta < 0$, $I > 0$, $J > 0$. As the angle θ is increasing, the shape of the ellipses of intersection is drastically changing. For $\theta = 0°$, since S_1 coincides with $O\sigma_1$, one axis of the ellipse is along $O\sigma_1$; if $A_{11} < A_{22}$, the eccentricity is: $e_0 = 2\sqrt{(A_{22} - A_{11})/(A_{44})}$, whereas if $A_{11} > A_{22}$, it is $e_0 = 2\sqrt{(A_{11} - A_{22})/(3A_{11})}$. For $\theta = 45°$, one axis of the ellipse is inclined at 60° to Oy; if $A_{22} < A_{55}/3$ the eccentricity is: $e_{45} = \sqrt{(A_{55} - 3A_{22})/A_{55}}$, while for $A_{22} > A_{55}/3$, the eccentricity is: $e_{45} = \sqrt{(A_{55} - 3A_{22})/3A_{22}}$. For $\theta = 90°$, one axis is along $O\sigma_3$; as expected $e_{90} = e_0$. As an example, in Fig. 2 are shown the cross-sectional shapes in the octahedral plane of the AMS surfaces for $A_{11} < A_{22}$, $a_1 < a_2$, and for $\theta = 0°$, 45°, and 90°, respectively; $\bar{\sigma}_i$ are the projections on the octahedral plane of the σ_i axes.

For any orientation θ, the axis of the elliptic paraboloid is piercing the octahedral plane in the center of the ellipse of intersection (0, y_C, z_C), where $y_C = (hF - BG)/J$, and $z_C = (hG - AF)/J$. Thus, the distance $|d_1(\theta)|$ from the vertex of the paraboloid to the octahedral plane is obtained by

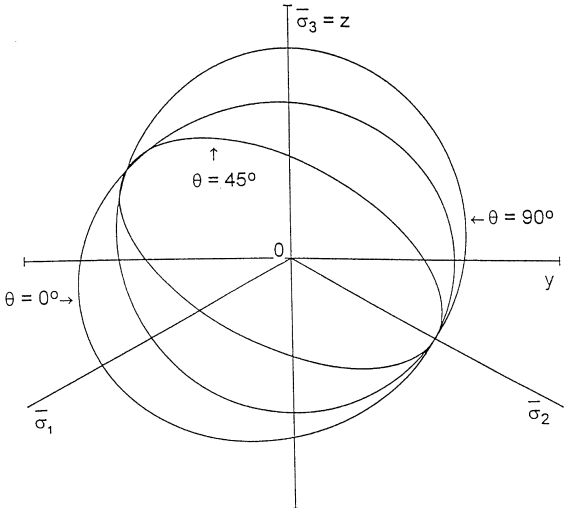

Fig. 2. Cross-sectional shapes in the octahedral plane of AMS failure surfaces corresponding to $\theta = 0°$, $\theta = 45°$, and $\theta = 90°$ ($A_{11} < A_{22}$, $a_1 < a_2$).

putting in Eq. (9) $x = 0$, $y = y_C$, and $z = z_C$. It follows that:

$$d_1(\theta) = -\frac{(a_2 - a_1)^2}{12J} \times \left[-(A_{44} - A_{55})(\sin(2\theta))^2/4 + A_{44} \right] - 1. \tag{13}$$

On the other hand, using Eqs. (6) and (7) we obtain that the hydrostatic strength of the material is:

$$\sigma_T = \frac{1}{2a_2 + a_1} = \frac{1}{2(1/Y_c - 1/Y_T) + (1/X_C - 1/X_T)}.$$

Since for rocks $X_T < X_C$, and $Y_T < Y_C$ follows that $\sigma_T < 0$, the failure surface being closed on the tensile side. Obviously, the distance between the origin O, and the point where the hydrostatic axis intersects the paraboloid is $|d|$, where

$$d = \sqrt{3}\sigma_T. \tag{14}$$

The difference between these two distances, $|d_1(\theta)| - |d|$, can be considered to be a measure of the "flatness" of the AMS surfaces.

Any intersection of the AMS surfaces by planes $x = constant$ are ellipses. In Fig. 3 are shown the intersections of the AMS surfaces for $A_{11} < A_{22}$, $a_1 < a_2$ by the octahedral plane, and three other planes parallel to it: $x = -d$, $x = d$, and $x = d/2$. Fig. 3(a) corresponds to the case when the principal strength axes coincide with the principal stress axes ($\theta = 0°$), while Fig. 3(b) and (c) correspond to off-axis loadings by angles $\theta = 45°$ and $\theta = 90°$, respectively. Obviously, for $x = d$, the elliptic intersections of AMS surfaces by this plane should pass through the origin O.

3.2. The AMS failure surface in triaxial plane

Because rock specimens are often submitted to a triaxial stress state in which two of the principal stresses are equal (such as uniaxial compression and tension tests, triaxial compression and extension tests), it is worthwhile to analyze the intersection of the AMS criterion with the usual triaxial plane. The AMS criterion is expressed in the principal stress system (X_1, X_2, X_3) by:

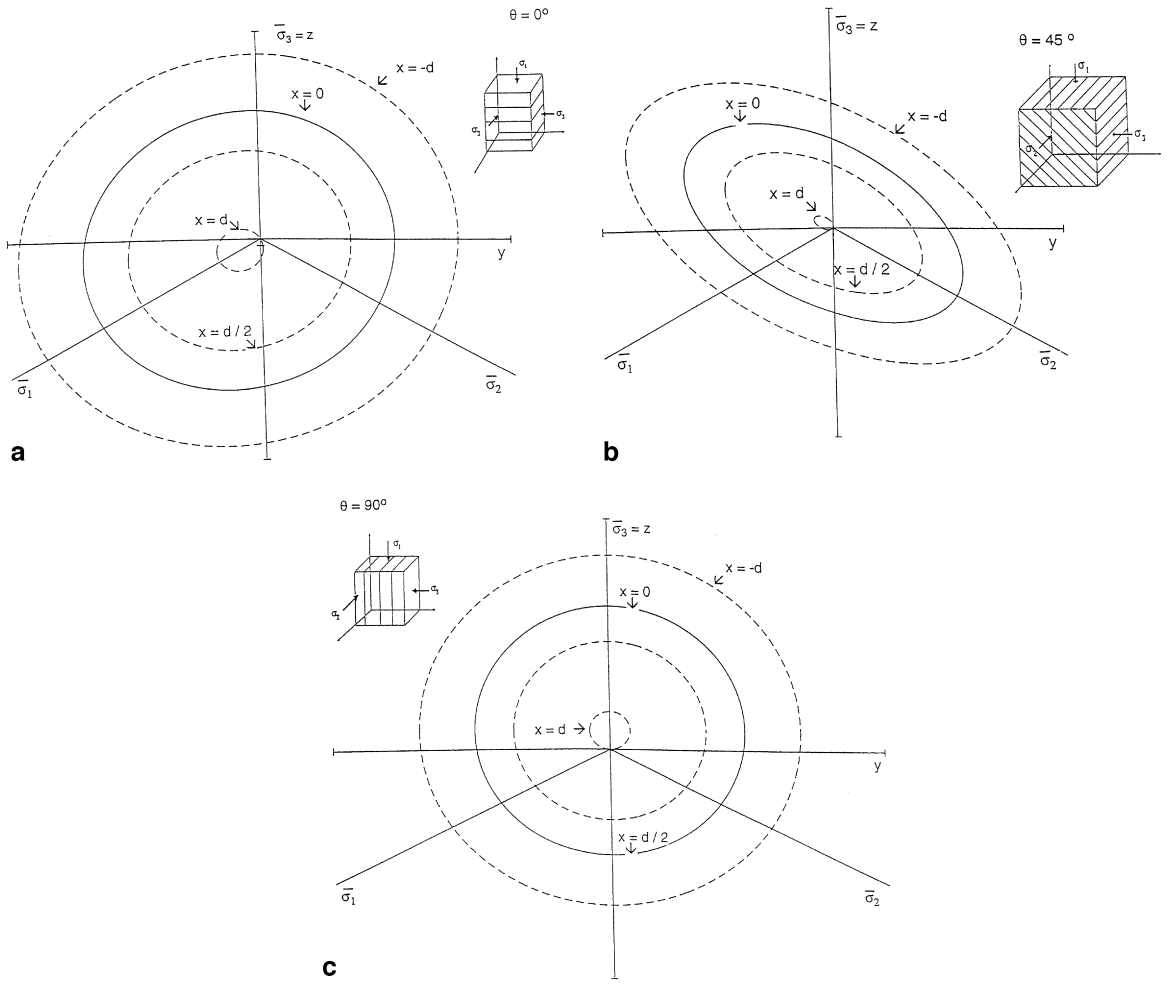

Fig. 3. Variation of cross-sectional shapes in deviatoric planes for AMS failure surfaces corresponding to diatomite for: (a) $\theta = 0°$; (b) $\theta = 45°$; (c) $\theta = 90°$ ($A_{11} < A_{22}$, $a_1 < a_2$).

$$a'_1\sigma_1 + a'_2\sigma_2 + a'_3\sigma_3 + A'_{11}\sigma_1^2 + A'_{22}\sigma_2^2 + A'_{33}\sigma_3^2 + 2A'_{12}\sigma_1\sigma_2 + 2A'_{13}\sigma_3\sigma_1 + 2A'_{23}\sigma_2\sigma_3 = 1. \quad (15)$$

The expressions of the new coefficients A'_{ij} and a'_i, in terms of the coefficients A_{ij}, a_i and the angle θ are given in the Appendix A. The equation expressing the intersection of the AMS criterion with the plane $(\sigma_3, \sqrt{2}\sigma_1 = \sqrt{2}\sigma_2)$, is defined by putting in Eq. (15), $\sigma_1 = \sigma_2$:

$$\alpha' u^2 + \beta'\sigma_3^2 + 2\delta' u\sigma_3 + 2\gamma' u + 2\eta'\sigma_3 - 1 = 0, \quad (16)$$

where

$$u = \sqrt{2}\sigma_1,$$
$$\alpha' = (1/2)(A'_{11} + A'_{22} + 2A'_{12}),$$
$$\beta' = A'_{33},$$
$$\delta' = (1/\sqrt{2})(A'_{13} + A'_{23}),$$
$$\gamma' = (1/(2\sqrt{2}))(a'_1 + a'_2),$$
$$\eta' = (1/2)a'_3. \quad (17)$$

For any orientation θ the conic Eq. (16) is a parabola. Indeed, $J' = \alpha'\beta' - \delta'^2 = 0$, and

$$\Delta' = \begin{bmatrix} \alpha' & \delta' & \gamma' \\ \delta' & \beta' & \eta' \\ \gamma' & \eta' & -1 \end{bmatrix}$$
$$= -\frac{(a_1+2a_2)^2}{32}\left\{\left[3(\cos\theta)^2-2\right]^2 A_{11} + A_{44}(\cos\theta)^4 + 2A_{55}(\sin 2\theta)^2\right\}.$$

The failure locus is "open" on the compressive side, showing that the axial pressure may be increased without limit, if the confining pressure is increased proportionally. However, the failure curve is "closed" on the tensile side and failure can occur under the tensile hydrostatic pressure

$$\sigma_T = \frac{1}{2a_2+a_1} = \frac{1}{2(1/Y_c - 1/Y_T) + (1/X_C - 1/X_T)}.$$

If $2X_T < Y_C$, then, $|\sigma_T| < Y_T$. Similarly, if condition $2Y_T < Y_C$ is satisfied then: $|\sigma_T| < X_T$. Thus, the hydrostatic absolute value of the hydrostatic tensile strength $|\sigma_T|$, is lower than Y_T and/or X_T. Although many existing criteria consider that the hydrostatic tensile strength should reduce to the uniaxial tensile strength, it seems more realistic that the application of multiaxial tensile stresses on rock reduces the value of the failure strength (see for example, Aubertin and Simon, 1997). Furthermore, a smooth failure curve avoids the physically unlikely angular apex found in the principal stress produced by the "tension cutoffs". Thus, the application of the AMS criterion to boundary-value problems is straightforward, since the surface is defined by a unique expression in the three-dimensional stress space.

As an example, in Fig. 4 is shown the intersection of the failure surface with the plane $\sigma_1 = \sigma_2$, for $\theta = 0°$, and $\theta = 90°$, for a diatomite (data after Allirot and Boehler, 1979). The intersections of the parabola corresponding to $\theta = 0°$ with the σ_3 axis are at the uniaxial compressive strength (Y_C), and the uniaxial tensile strength ($-Y_T$), respectively. Point C represents the limiting loading condition for a hydrostatic tensile stress state. The intersections with the ($\sigma_1 = \sigma_2$, $\sigma_3 = 0$) axis represent the biaxial failure strengths in compression and tension, respectively. Similarly, for $\theta = 90°$, the intersections with the σ_3 axis are the uniaxial

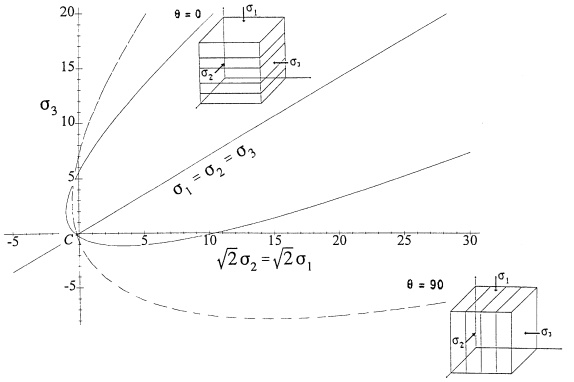

Fig. 4. Intersection of the AMS criterion with the triaxial plane (σ_3, $\sqrt{2}\sigma_1 = \sqrt{2}\sigma_2$) for $\theta = 0°$, and $\theta = 90°$ (data after Allirot and Boehler, 1979).

compressive strength (X_C), and the uniaxial tensile strength ($-X_T$), respectively. The parabola passes through the same point C, expressing that hydrostatic strength does not depend on the orientation of the applied loading with respect to the structural axis of the material. The biaxial compressive strength for $\theta = 90°$ is of 51 MPa and it is not represented on Fig. 4.

The results of triaxial compression tests and extension tests may conveniently be shown in the (p,q) plane, where $p = I_1/3$, and $q = \sqrt{3J_2}$. For a given orientation θ, the failure curve corresponding to conventional triaxial compression (CTC) tests ($\sigma_1 = \sigma_2 < \sigma_3$) is a parabola of equation:

$$BB(\theta)q^2 + 2gp + 2f_1(\theta)q - 1 = 0, \tag{18}$$

with

$$BB(\theta) = (2A_{11} + A_{22} - A_{55})(\cos\theta)^4 + (A_{55} - 3A_{11})(\cos\theta)^2 + A_{11},$$
$$g = \frac{a_1+2a_2}{2},$$
$$f_1(\theta) = \frac{(a_1-a_2)(3(\cos\theta)^2-2)}{6}. \tag{19}$$

On the other hand, in reduced triaxial extension (RTE) tests ($\sigma_1 < \sigma_2 = \sigma_3$) the failure curve is a parabola of equation:

$$BB(\theta)q^2 + 2gp + 2f_2(\theta)q - 1 = 0 \tag{20}$$

with

$$f_2(\theta) = -\frac{(a_1 - a_2)(\cos\theta)^2}{2} + \frac{a_1 - 4a_2}{6}. \tag{21}$$

The intersection with the q axis of the CTC parabola is at:

$$q_{CTC} = \frac{-f_1(\theta) + \sqrt{f_1(\theta)^2 + BB(\theta)}}{BB(\theta)}, \tag{22}$$

whereas the RTE parabola intersects the q axis at

$$q_{RTE} = \frac{-f_2(\theta) + \sqrt{f_2(\theta)^2 + BB(\theta)}}{BB(\theta)}. \tag{22'}$$

The intersections of both parabolas with the p axis are at the hydrostatic tensile strength $\sigma_T = 1/(2a_2 + a_1)$. Since $BB(\theta) > 0$ for any θ, it follows that $q_{CTC} > q_{RTE}$. Thus, in the case when the intermediate principal stress σ_2 is oriented parallel to the symmetry planes, for any orientation θ, the predicted strength in CTC conditions ($\mu_\sigma = -1$) is higher than in RTE conditions ($\mu_\sigma = 1$), where $\mu_\sigma = (2\sigma_2 - \sigma_1 - \sigma_3)/(\sigma_1 - \sigma_3)$ is the Nadai-Lode parameter. As an example, in Fig. 5 are shown the RTE and CTC parabolas for $\theta = 45°$, the parameters being determined for the Texas slate (data after McLamore and Gray, 1967). The solid lines correspond to the predictions of the AMS criterion, while the experimental points are represented by symbols. No RTE test results were available.

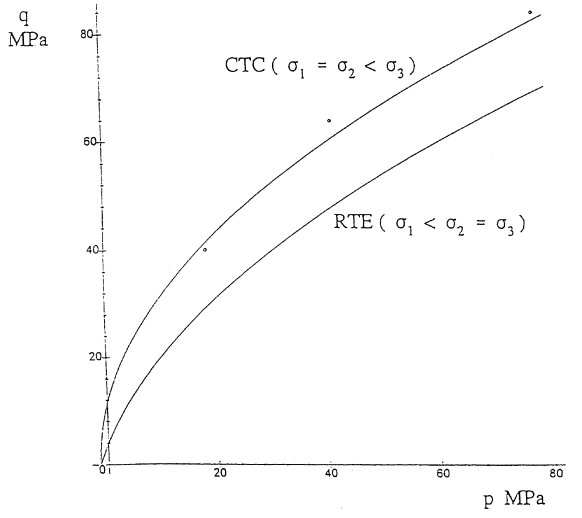

Fig. 5. Representation of the AMS criterion in the (p,q) plane showing the influence of the magnitude of the intermediate principal stress on strength (data after McLamore and Gray, 1967).

This effect of the magnitude of the intermediate stress on the strength of transversely isotropic rocks has been experimentally observed for clay shales (e.g., Beron and Chirkov, 1969; Niandou et al., 1997). The CTC and RTE tests are, however, insufficient to assess the strength properties of the rock at intermediate stresses different from σ_3 and σ_1, and thus under conditions when $-1 < \mu_\sigma < 1$.

3.3. AMS failure surface in biaxial plane

Biaxial tests supply additional information on the effect of the magnitude of the intermediate principal stress σ_2 on the strength properties of rock. The results of such tests, in which one of the principal stresses is zero, may conveniently be shown in a biaxial plane. The equation expressing the intersection of the AMS failure surface with the biaxial plane is readily defined by putting in Eq. (15), $\sigma_1 = 0$:

$$A'\sigma_2^2 + 2H'(\theta)\sigma_2\sigma_3 + BB(\theta)\sigma_3^2 + 2g'\sigma_2 + 2f'(\theta)\sigma_3 - 1 = 0, \tag{23}$$

where

$$A' = A_{22},$$
$$H'(\theta) = (A_{11} - A_{22})(\cos\theta)^2 - A_{11}/2,$$
$$g' = -a_2/2,$$

$$BB(\theta) = (2A_{11} + A_{22} - A_{55})(\cos\theta)^4 + (A_{55} - 3A_{11})(\cos\theta)^2 + A_{11},$$
$$f'(\theta) = \left[a_1 - (a_1 - a_2)(\cos\theta)^2\right]\Big/2. \tag{24}$$

For any orientation θ, Eq. (23) is an ellipse. For $\theta = 0°$, that corresponds to the case when the principal stress directions σ_2 and σ_3 belong to the isotropy plane (S_2, S_3), the intersections of this ellipse with the σ_3 axis as well as with the σ_2 axis are at the uniaxial compressive strength (Y_C), and at the uniaxial tensile strength ($-Y_T$), respectively. The intersections with the symmetry axis $\sigma_2 = \sigma_3$ represent the biaxial strength in compression and tension, respectively. Thus, the predicted absolute

value of the biaxial tensile strength is higher than the uniaxial tensile strength. Similarly, for $\theta = 90°$ that corresponds to the case when the maximum principal stress σ_3 is oriented perpendicular to the symmetry planes, the intersection with the σ_3 axis are at the uniaxial compressive strength (X_C), and at the uniaxial tensile strength ($-X_T$), whereas the intersections with the σ_2 axis are at the uniaxial compressive strength (Y_C), and at the uniaxial tensile strength ($-Y_T$), respectively. The slope of the axis of symmetry is:

$$m_{90} = -X_C X_T \left(\frac{1}{X_C X_T} - \frac{1}{Y_C Y_T} + \sqrt{\left(\frac{1}{X_C X_T} - \frac{1}{Y_C Y_T} \right)^2 + \frac{1}{X_C^2 X_T^2}} \right). \quad (25)$$

As an example, in the following we will apply the AMS criterion to a metamorphic limestone using the biaxial compression data obtained by Dayre and Sirieys (1965). In the experiments, the maximal stress σ_3 was oriented either perpendicular or parallel to the schistosity planes, but the direction of the intermediate principal stress σ_2 remained parallel to the schistosity. Fig. 6 shows the AMS failure curves in biaxial compression (i.e., the portions of the ellipses of intersection above $\sigma_2 = \sigma_3$) for $\theta = 0°$, and $\theta = 90°$. Although the scatter in the data is great, the AMS criterion reproduces qualitatively the fact that the strength of the rock is dependent to a much greater degree on the orientation of the maximum stress to the symmetry planes than on the magnitude of σ_2.

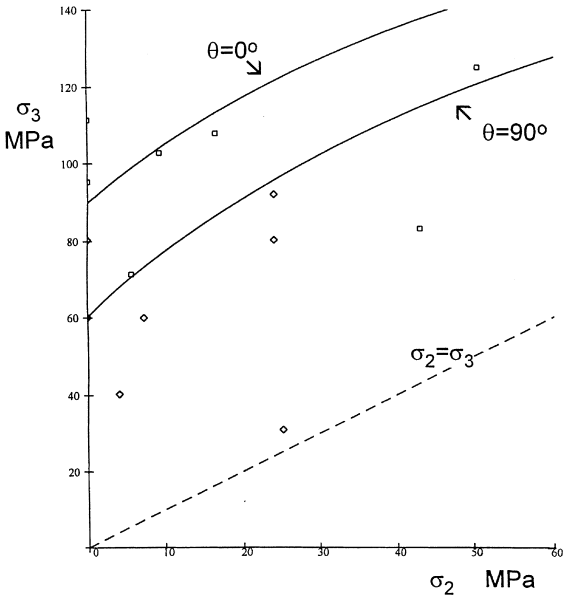

Fig. 6. Dependence of the limiting maximum principal stress σ_3 on the intermediate principal stress σ_2 for a limestone, with σ_3 oriented perpendicular (□) and parallel to the symmetry (◇) planes (data after Dayre and Sirieys, 1965).

3.4. Comparison with experimental data in conventional triaxial compression

The determination of the material parameters of the AMS criterion from simple laboratory tests is straightforward. Indeed, the expressions of the coefficients of the AMS criterion in terms of engineering strengths are given by Eq. (7). The additional condition $1/Q^2 = 4/(Y_T Y_C) - 1/X_C$ implies that the shear strength in the isotropy plane (S_2, S_3) is defined directly in terms of the uniaxial strengths of the material. Thus, for the determination of the parameters of the AMS criterion, only two types of tests need to be performed: (a) uniaxial compression and uniaxial tensile tests in the S_1 and S_2 direction, respectively; (b) shear test in the (S_1, S_2) plane. Since for rocks shear tests are very difficult to perform and to interpret, the parameter c can be estimated by least square fit using the compression strengths at a given confining pressure for the orientations $\theta = 0°$ and $\theta = 90°$, and at least another intermediate orientation.

In the following, we will apply the AMS criterion to several transversely isotropic rocks, and compare the theoretical predictions to the data from conventional triaxial compression tests. Consider first the experimental data on Tournemire shale obtained in Lille Mechanics laboratory by Niandou (1994). The rock is an upper Toarcian massive shale. At the macroscopical level, the rock is characterized by a well defined stratified structure. Ultrasonic measurements carried out on cubical specimens have shown that this rock exhibits intrinsic transverse isotropy (see Homand et al., 1993). This type of anisotropy is conserved up to failure, as shown by the compression test results (see Niandou, 1994). Five replications of each test

were performed. For Tournemire shale, the mean arithmetic value of X_C is 48 MPa, whereas $Y_C = 50$ MPa. No tensile test results were available. We assumed that: $X_T = 3.92$ MPa, and $Y_T = 4.1$ MPa, the estimate being based on data on oily shales reported by other researchers (see Lama and Vutukuri, 1978). For the estimation of the parameter c the test results at a confining pressure of 50 MPa for the orientations $\theta = 0°$, 30°, 45°, 60° and 90° were used. The numerical values obtained for the coefficients are: $a = 1.205$ MPa^{-1}, $b = 1.13529$ MPa^{-1}, $c = 0.098$ MPa^{-1}, $d = 3.517$ MPa^{-1}, $e = -1.325$ MPa^{-1} and $m = 4.613$ MPa^{-1}. Fig. 7 shows the variation of the peak axial stress σ_a with the orientation θ for several confining pressures. The solid lines correspond to the predictions of the AMS criterion, while the experimental points are represented by symbols. The experimental results show that for each confining pressure the minimum strength is found between $\theta = 45°$ and $\theta = 50°$ while two maximum values of the strengths are obtained for $\theta = 0°$ and $\theta = 90°$. As a general remark, the strength anisotropy is decreasing as the confining pressure is increasing. For the AMS criterion the comparison with the data is successful in the whole. The influence of the confining pressure on the strength characteristics is well described although only the test results for $p_c = 50$ MPa were used for the determination of the parameter c.

The AMS criterion was also applied to Martinsburg slate, using the experimental data obtained by Donath (1964, 1972). The rock presents a pervasive planar anisotropy. No uniaxial test results were available. We assumed that: $X_T = 6.8$ MPa, and $Y_T = 7$ MPa. By extrapolating the data shown in Fig. 8 toward $\theta = 0°$ and $\theta = 90°$, we have found that: $X_C = 290$ MPa, and $Y_C = 200$ MPa. To evaluate the coefficient c, we used the experimental confined compression strengths at $p_c = 100$ MPa ($p_c = 1000$ bars), for θ ranging from 0° to 90° at 15° interval. By least square fit we obtained: $c = 0.058$ MPa^{-1}, while by making use of Eq. (7), we estimated: $a = 0.39$ MPa^{-1}, $b = 0.367$ MPa^{-1}, $d = 6.311$ MPa^{-1}, $m = 9.183$ MPa^{-1} and $e = -6$ MPa^{-1}. In Fig. 8 the calculated curves are plotted together with the experimental results. The data points are the average values of the strengths reported by Donath (1964). The AMS criterion describes well the effect of planar anisotropy on the strength of rock over the entire range of confining pressures. For lower confining pressures the experimental results are better matched for

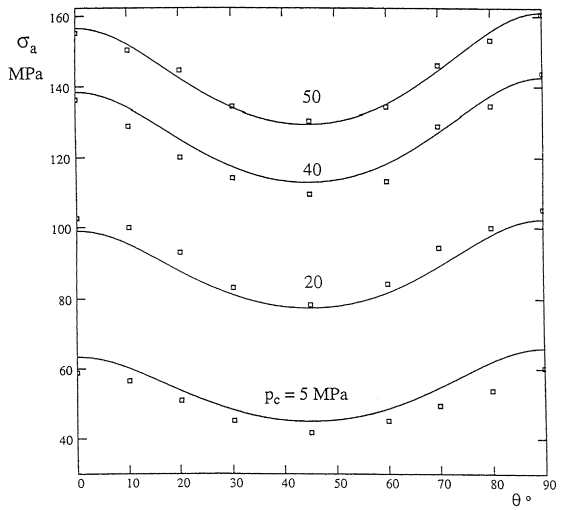

Fig. 7. The AMS criterion applied to Tournemire shale (data after Niandou, 1994).

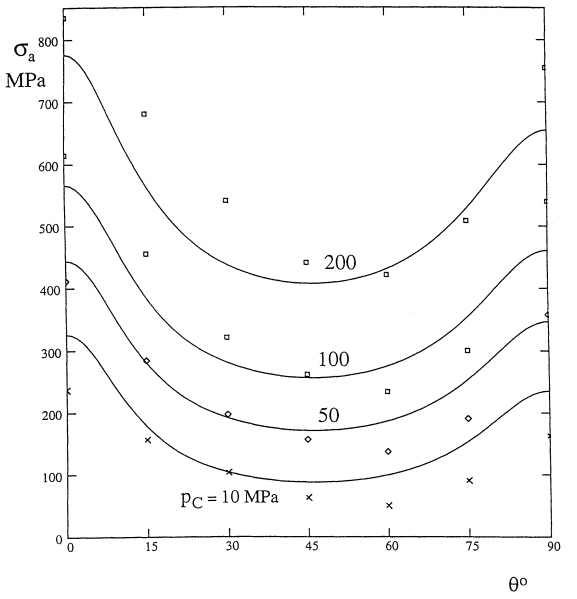

Fig. 8. Strength variation of Martinsburg slate (symbols) as a function of anisotropy orientation, compared with theoretical curves (data after Donath, 1972).

$\theta \in (0°, \theta_C)$, θ_C corresponding to the minimum value of the fracture strength, while for higher confining pressures a better agreement is obtained for θ higher than θ_C. The less good agreement for $\theta = 90°$ may be due to the restraining effect of the piston and anvil that prevent failure by simple shear fracture (see Donath, 1972).

The theoretical predictions for Penrhyn slate (data after Attewell and Sandford, 1974) are plotted in Fig. 9. Ultrasonic and X-ray crystallographic measurements show that this rock is transversely isotropic about an axis normal to the cleavage. The experimental data points for $p_c = 13.789$ MPa, $p_c = 27.579$ MPa, $p_c = 41.368$ MPa and $p_c = 55.158$ MPa are represented by symbols. For the identification of the parameter c, the experimental values of the confined strengths at $p_c = 41.368$ MPa were used. Following the procedure outlined we obtained: $c = 0.002$ MPa^{-1}, $a = 0.78$ MPa^{-1}, $b = 0.768$ MPa^{-1}, $d = 14.544$ MPa^{-1}, $e = -13.02$ MPa^{-1}, $m = 3.438$ MPa^{-1}. The criterion reproduces the trend shown by the experimental data.

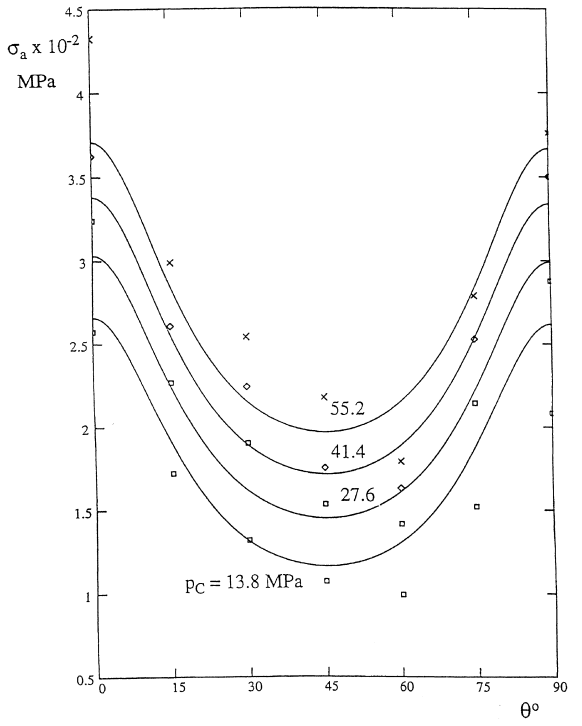

Fig. 9. Comparison between theoretical and experimental results on Penrhyn slate (data after Attewell and Sandford, 1974).

4. Conclusion

The characteristics of failure surfaces for transversely isotropic intact rocks under both tensile and compressive stresses are captured by a general three-dimensional failure criterion formulated in terms of the first and second invariant of a transformed stress tensor. The criterion is written in a coordinate-free form and thus can be easily applied for any orientation of the principal stress axes with respect to the structural system associated with the material intrinsic symmetry. It predicts that the application of multiaxial tensile stresses on rock reduces the value of the failure strength, i.e., the predicted value of the hydrostatic tensile strength as well as of the biaxial tensile strength is less than the uniaxial tensile strength in any direction. The intersections of the AMS failure surfaces with the octahedral plane demonstrates the ability of the criterion to describe the directional character of the strength of transversely isotropic rock under general loading conditions. The application of the criterion to conventional triaxial compression conditions, reduced triaxial extension, and biaxial compression show that the criterion captures the influence of the magnitude of the intermediate principal stress on strength. This failure criterion involves a few number of parameters that are directly expressible in terms of the engineering strengths of the material. The procedure for the identification of these parameters from simple tests was outlined. Representative sets of data on transversely isotropic intact rock have been analyzed, and comparison between the theoretical predictions appears to be reasonably good.

Appendix A

Assume that the applied principal stresses coordinate system (X_1, X_2, X_3) is such that $X_2 || S_2$, and S_1 is obtained from X_1 by rotation about S_2 with the angle θ. In this coordinate system the AMS criterion is expressed by:

$$a'_1\sigma_1 + a'_2\sigma_2 + a'_3\sigma_3 + A'_{11}\sigma_1^2 + A'_{22}\sigma_2^2 + A'_{33}\sigma_3^2 + 2A'_{12}\sigma_1\sigma_2 + 2A'_{13}\sigma_3\sigma_1 + 2A'_{23}\sigma_2\sigma_3 = 1. \quad (A.1)$$

The coefficients A'_{ij} and a'_i are expressed in terms of the coefficients A_{ij}, a_i and the angle Θ by (see Cazacu et al., 1998):

$$\begin{aligned}
A'_{11} &= A_{11}\cos^4\theta + A_{22}\sin^4\theta \\
&\quad + (2A_{12} + A_{55})\sin^2\theta\cos^2\theta, \\
A'_{22} &= A_{22}, \\
A'_{33} &= A_{11}\sin^4\theta + A_{22}\cos^4\theta \\
&\quad + (2A_{12} + A_{55})\sin^2\theta\cos^2\theta, \\
A'_{12} &= A_{23}\sin^2\theta + A_{12}\cos^2\theta, \\
A'_{13} &= (A_{11} + A_{22} - A_{55} - 2A_{12})\sin^2\theta\cos^2\theta + A_{12}, \\
A'_{23} &= A_{12}\sin^2\theta + A_{23}\cos^2\theta, \\
a'_1 &= a_1\cos^2\theta + a_2\sin^2\theta, \\
a'_2 &= a_2, \\
a'_3 &= a_1\sin^2\theta + a_2\cos^2\theta. \quad (A.2)
\end{aligned}$$

References

Allirot, D., Boehler, J.P., 1979. In: Proceedings of the Fourth International Society of Rock. Mechanics 1, Montreux, Balkema, Rotterdam, pp. 15–22.

Attewell, B., Sandford, M.R., 1974. Intrinsic shear strength of a brittle anisotropic rock. I. Experimental and mechanical interpretation. II. Textural data acquisition and processing. III. Textural interpretation of failure. Int. J. Rock. Mech. Min. Sci. 11, 423–451.

Aubertin, M., Simon, R., 1997. A damage initiation criterion for low porosity rocks. Int. J. Rock. Mech. Min. Sci. and Geomech. Abstr., 34, in press.

Beron, A.I., Chirkov, S.E., 1969. Study of strength of rocks under conditions of triaxial non-uniform compression. Nauch. Soobshch. Inst. Gorn. Dela Im. A.A. Skochinskogo 61, 33–38.

Boehler, J.P., Sawczuk, A., 1977. On yielding of oriented solids. Acta Mechanica 27, 185–206.

Boehler, J.P., 1978. Lois de comportement anisotrope des milieux continus. Journal deMécanique 17, 153–190.

Boehler, J.P., 1987. Yielding and failure of transversely isotropic solids, In: Boehler, J.P. (Ed.), Applications of tensor functions in Solid Mechanics, CISM Courses and Lectures No 292. Springer, Berlin, pp. 3–140.

Cazacu, O., Cristescu, N.D., Shao, J.F., Henry, J.P., 1998. A new anisotropic failure criterion for transversely isotropic solids. Mech. Cohes. Frict. Mater. 3, 89–103.

Chenevert, M.E., Gatlin, C., 1965. Mechanical anisotropies of laminated sedimentary rocks. Soc. Petrol. Eng. J. 5, 67–77.

Cowin, S.C., 1979. On the strength anisotropy of bone and wood. J. Appl. Mech. 46, 832–836.

Dayre, M., Sirieys, P.M., 1965. Anisotropie des modules élastiques et des résistances à la rupture des roches métamorphiques. C.R. Acad. Sci. Paris 260, 4440–4443.

Donath, F.A., 1964. Strength variation and deformational behavior in anisotropic rock. In: Judd, W.R. (Ed.), State of Stress in the Earth's Crust. Elsevier, Amsterdam, pp. 281–297.

Donath, F.A. (1972). Effects of cohesion and granularity on deformational behavior of anisotropic rock. In: Doc B.R., Smith, D.K. (Eds.), Studies in Mineralogy and Precambrian Geology, Geological Society of America, Boulder, vol. 135, pp. 95–128.

Hill, R., 1948. A theory of yielding and plastic flow of anisotropic metals. In: Proceeding of the Royal Society, London, Ser. A, vol. 193, pp. 281–297.

Homand, F., Morel, E., Henry, J.P., Cuxac, P., Hammade, E., 1993. Characterization of the moduli of elasticity of an anisotropic rock using dynamic and static methods. Int. J. Rock. Mech. Min. Sci and Geomech. Abstr. 30, 527–535.

Jaeger, J.C., 1960. Shear failure of anisotropic rocks. Geol. Mag. 97, 65–72.

Labossière, P., Neale, K.W., 1987. Macroscopic failure criteria for fibre-reinforced composite materials. SM Archiv. 12, 65–95.

Lama, R.D., Vutukuri, V.S., 1978. Handbook on mechanical properties of rocks, vol. II: Testing Techniques and Results, Trans. Tech. Publ., pp. 57–148, 254–282.

Liao, J.J., Yang, M-T., Hsieh, H-Y., 1997. Direct tensile behavior of transversely isotropic rock. Int. J. Rock Mech. Min. Sci. and Geomech. Abstr. 34, 837–851.

Lubliner, J., 1990. Plasticity Theory. Macmillan, New York.

McLamore, R., Gray, K.E., 1967. The mechanical behavior of anisotropic sedimentary rocks. J. Eng. Ind., Trans. of the ASME, 89, 62–73.

Niandou, H., 1994. Étude du comportement rhéologique et modélisation de l'argilite de Tournemire. Application à la stabilité des ouvrages souterrains, Ph.D. Thesis, USTL, Univérsité de Lille 1.

Niandou, H., Shao, J.F., Henry, J.P., Fourmaintraux, D., 1997. Laboratory investigation of the mechanical behaviour of Tournemire shale. Int. J. Rock Mech. Min. Sci. and Geomech. Abstr. 34, 3–16.

Nova, R., 1980. The failure of transversely anisotropic rocks in triaxial compression. Int. J. Rock. Mech. Min. Sci. and Geomech. Abstr. 17, 325–332.

Nova, R., Zaninetti, A., 1990. An investigation into the tensile behaviour of a schistose rock. Int. J. Rock Mech. Min. Sci. 27 (4), 231–242.

Pariseau, W.G., 1972. Plasticity theory for anisotropic rocks and soils, In: Proceedings of the Tenth Symposium on Rock Mechanics, AIME, pp. 267–295.

Ramamurthy, T., 1993. Strength and modulus responses of anisotropic rocks, In: Hudson, J.A. (Ed.), Comprehensive

Rock Engineering. Pergamon Press, Oxford, 1, pp. 313–329.

Theocaris, P.S., 1991. The elliptic paraboloid failure criterion for cellular solids and brittle foams. Acta Mechanica 89, 93–121.

Tsai, S.M., Hahn, H.T., 1980. Introduction to composite materials, Technomic Publishing Co, Westport, Connecticut.

Tsai, S.M., Wu, E., 1971. A general theory of strength of anisotropic materials. J. Composite Mater. 5, 58–80.

Wu, R.Y., Stachurski, Z., 1984. Evaluation of the normal stress interaction parameter in the tensor polynomial theory for anisotropic materials. J. Composite Mater. 18, 456–463.